Biosensors and Bioelectronics 226 (2023) 115137

Contents lists available at ScienceDirect

Biosensors and Bioelectronics

journal homepage: www.elsevier.com/locate/bios

Biomimetic nanoplasmonic sensor for rapid evaluation of neutralizing SARS-CoV-2 monoclonal antibodies as antiviral therapy

Razia Batool [a], Maria Soler [a,*], Francesca Colavita [b], Lavinia Fabeni [b], Giulia Matusali [b], Laura M. Lechuga [a,**]

[a] Nanobiosensors and Bioanalytical Applications Group (NanoB2A), Catalan Institute of Nanoscience and Nanotechnology (ICN2), CSIC, BIST, CIBER-BBN, Spain
[b] National Institute for Infectious Disease "L. Spallanzani", IRCCS, Rome, Italy

ARTICLE INFO

Keywords:
Surface plasmon resonance
COVID-19
Immunotherapy
Neutralization assay
Supported lipid bilayer
Label-free analysis

ABSTRACT

Monoclonal antibody (mAb) therapy is one of the most promising immunotherapies that have shown the potential to prevent or neutralize the effects of COVID-19 in patients at very early stages, with a few formulations recently approved by the European and American medicine agencies. However, a main bottleneck for their general implementation resides in the time-consuming, laborious, and highly-specialized techniques employed for the manufacturing and assessing of these therapies, excessively increasing their prices and delaying their administration to the patients. We propose a biomimetic nanoplasmonic biosensor as a novel analytical technique for the screening and evaluation of COVID-19 mAb therapies in a simpler, faster, and reliable manner. By creating an artificial cell membrane on the plasmonic sensor surface, our label-free sensing approach enables real-time monitoring of virus-cell interactions as well as direct analysis of antibody blocking effects in only 15 min assay time. We have achieved detection limits in the 10^2 TCID50/mL range for the study of SARS-CoV-2 viruses, which allows to perform neutralization assays by only employing a low-volume sample with common viral loads. We have demonstrated the accuracy of the biosensor for the evaluation of two different neutralizing antibodies targeting both Delta and Omicron variants of SARS-CoV-2, with half maximal inhibitory concentrations (IC_{50}) determined in the ng/mL range. Our user-friendly and reliable technology could be employed in biomedical and pharmaceutical laboratories to accelerate, cheapen, and simplify the development of effective immunotherapies for COVID-19 and other serious infectious diseases or cancer.

1. Introduction

Since December 2019, research in coronavirus infectious disease (COVID-19) has become a hot topic in the field of sensors and analytical techniques for diagnostics as well as in vaccine and therapy development. COVID-19, caused by the SARS-CoV-2 (Severe Acute Respiratory Syndrome Coronavirus 2), was declared a pandemic by the World Health Organization (WHO) in early 2020 (Hadi et al., 2020; Mohan and Vinod, 2020; Sheervalilou et al., 2020), with a rapid worldwide spread that accumulates hundreds of million cases and millions of deaths (Sen-Crowe et al., 2020). Furthermore, the COVID-19 pandemic has seriously challenged many healthcare systems with a drastic work overload and a lack of resources to provide rapid diagnostic and prognostic information, and novel treatments for effective patient management (Kevadiya et al., 2021; Ludwig and Zarbock, 2020). Significant efforts have been made for the development and distribution of rapid detection tests (Dinnes et al., 2021; Singh et al., 2022; Thapa et al., 2022; Wang et al., 2020) and vaccines (Creech et al., 2021) that so far have successfully allowed an efficient population screening, slowing down viral transmission, and greatly reducing clinical complications and deaths by SARS-CoV-2 infection. However, the administration of antiviral therapies for an early treatment of the disease seems to have found significant difficulties, becoming a bottleneck in the clinical assistance.

Early antiviral therapies for COVID-19 are a critical need in high-risk individuals with comorbidities, weaken immune systems, or limited access to vaccination (AminJafari and Ghasemi, 2020; Wouters et al., 2021). Besides of the desired effectiveness to prevent and control SARS-CoV-2 infection with minimum side effects, they should be widely available, affordable, and suitable for non-hospitalized patients. Among different candidates, such as the convalescent plasma (Li et al., 2020) or

* Corresponding author.
** Corresponding author.
E-mail addresses: maria.soler@icn2.cat (M. Soler), laura.lechuga@icn2.cat (L.M. Lechuga).

https://doi.org/10.1016/j.bios.2023.115137
Received 14 October 2022; Received in revised form 16 January 2023; Accepted 6 February 2023
Available online 8 February 2023

the antivirals paxlovid and remdesivir (AminJafari and Ghasemi, 2020; Pashaei and Rezaei, 2020), the most promising ones have been the monoclonal antibody (mAb) immunotherapies (Pashaei and Rezaei, 2020). Monoclonal antibodies are recombinant or *in vitro* produced immunoglobulin proteins that mimic the immune system's ability to prevent and stop the coronavirus infection by binding to external viral spikes (S protein), inhibiting its interaction with the host cell receptors, and therefore neutralizing virus entry and replication in the human organism (Fig. 1) (AminJafari and Ghasemi, 2020). A few mAb therapies have been approved by the American Food and Drug Administration (FDA) and the European Medicine Agency (EMA) between 2021 and 2022 for the treatment of mild to moderate COVID-19 patients, like bamlanimivab, regdanvimab, sotrovimab, or the cocktails casirivimab/imdevimab and tixagevimab/cilgavimab (Drożdżal et al., 2020; Plaze et al., 2021). Nonetheless, their late approval and high prices evidence the challenging, laborious, and time-consuming procedures required to develop and evaluate antiviral mAb therapies, which could became a major limitation for their general implementation in health systems (Niknam et al., 2022; Sparrow et al., 2017). The selection and validation of mAb immunotherapies is generally carried out via neutralization assays (Payne, 2017). Initial steps of the protocol include high-throughput screening techniques to identify antibodies with high affinity toward the S protein (or its receptor binding domain, RBD), often performed with multiplexed bead-based assays (e.g., Luminex) or enzyme-linked immunosorbent assays (ELISA), among others. Once selected, antibodies are evaluated through an infectivity or neutralization assay. This assay consists in incubating the antibody at different titers with purified samples of the virus – usually employing a pseudotyped virus (Lei et al., 2020); and these samples are added to a dish of cultured cells representing the host. In the absence of neutralizing antibodies, the viruses will infect the host cells generating a number of plaques and areas lacking cells. At increasing antibody concentrations, their ability to block and neutralize virus infectivity will be measured by either counting the number of formed plaques or the inhibition of the cytopathic effect (i.e., microneutralization test), resulting in a titration curve from which the optimum dose and the half maximum inhibitory concentration (IC_{50}) are determined. The main drawbacks of this technique are the long times required for cell culture and plaque forming by viral infection that can extend from several hours to days. Also, the complexity, specialization, and laborious procedures for microbiology and cell culturing inevitably increase the costs and price of the therapy (Iacob and Iacob, 2020).

To overcome these limitations, we introduce a new biomimetic label-free plasmonic sensor for simplifying and accelerating the screening and evaluation of novel mAb immunotherapies for COVID-19. This novel sensing technology provides accurate, reliable, and precise neutralization information with a minimum sample and reagent consumption, rapid assays, and user-friendly operation. In particular, we propose the use of a Surface Plasmon Resonance (SPR) biosensor as a mature technology, worldwide commercially available, automatable, and with demonstrated reliability for pharmacology studies, diagnostics, and therapy evaluation applications (Nguyen et al., 2015; Soler and Huertas, 2022). SPR biosensor systems are based on the evanescent field sensing principle that enables the label-free monitoring of biochemical and biomolecular interactions in real time with excellent sensitivities (pM-nM range). Most common SPR sensors employ a nanometer-thin layer of gold (45–50 nm) as transducer, in which the propagating electromagnetic resonance (i.e., collective oscillation of conduction band electrons) is excited through prism-coupled illumination with a polarized light beam (Kretschmann configuration) (Soler and Lechuga, 2021). This plasmonic resonance generates the electromagnetic field that evanescently penetrates into the adjacent dielectric up to a few hundreds of nanometers (100–300 nm), probing the biomolecular interactions as a response to the variation of the refractive index of the medium. The

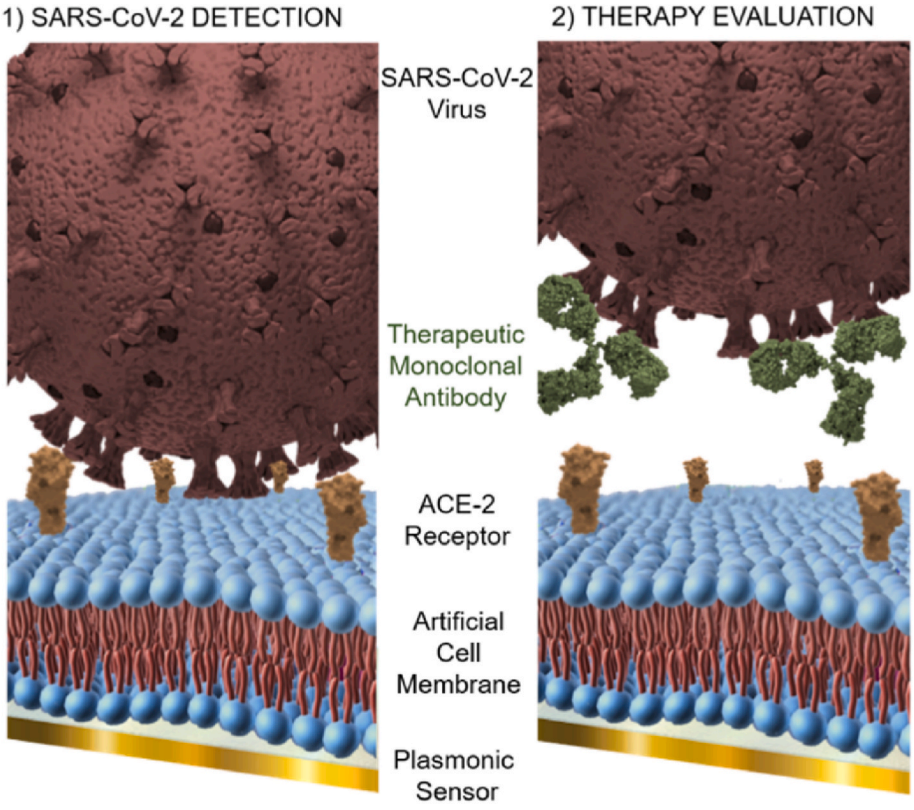

Fig. 1. Schematic illustration of the biomimetic plasmonic biosensor approach for mAb therapy evaluation via neutralization assays. 1) panel shows direct capture and detection of SARS-CoV-2 viruses over an artificial cell membrane displaying ACE-2 receptors created on the plasmonic sensor. 2) panel shows how therapeutic monoclonal antibodies bind to the Spike protein of the SARS-CoV-2 virus, blocking and inhibiting its interaction with the host cell.

interrogation of certain properties of the light, such as angle, intensity or wavelength, provides quantitative information about the concentration of the analyte captured on the sensor surface and also the affinity and kinetic parameters of the biomolecular interaction. In the last two years, plasmonic biosensors have been demonstrated for different applications in COVID-19, primarily for antigen- and antibody-targeted diagnostics, but also for the study of the biomolecular interactions involved in the SARS-CoV-2 infection cycle (Behrouzi and Lin, 2022; Hassan et al., 2021; Mauriz and Lechuga, 2021; Shrivastav et al., 2021; Syed Nor et al., 2022; Szunerits et al., 2022; Yano et al., 2022; Ye et al., 2021; Saad et al., 2022), with detection limits in the 1–100 ng/mL range for proteomic assays and 10^3–10^5 viruses/mL for cell and genomic analysis, and for the screening and profiling of therapy candidates, including antibodies (AminJafari and Ghasemi, 2020). However, these publications only address isolated biomolecular interactions, employing in-solution recombinant proteins with three-dimensional (3D) freedom that do not take into account the intrinsic cell physiology and microenvironment restrictions in terms of mobility and number of interactions (Soler et al., 2018).

The main novelty and innovation of our work reside on a two-dimensional (2D) biomimetic assay approach employed to increase the reliability and transferability of the therapy screening tests while reducing the analysis times and the overall complexity of the evaluation study. Our biosensor is functionalized with an artificial cell membrane displaying the host cell receptors utilized by the SARS-CoV-2 for entry and infection, i.e., the angiotensin-converting enzyme 2 (ACE2), and the neutralization assay is performed with ultraviolet (UV)-inactivated SARS-CoV-2 viruses, which maintain the structural properties and protein activity and can be safely manipulated in P2-level biosafety laboratory installations (Ruiz-Vega et al., 2022). With this methodology, we can more accurately simulate the virus-cell interaction during an infectivity assay – where both target molecules are anchored to their respective cell membranes - while eliminating the need of host cell culture procedures. Artificial cell membranes formed by planar lipid bilayers have been previously demonstrated and applied in biosensing for cell biology studies (e.g., protein-membrane interactions (Dahlin et al., 2005), for drug discovery research (Limaj et al., 2016), and also for the evaluation of cell immunotherapies for cancer (Soler et al., 2018). We take advantage of this unique biomimetic scaffold to attain and deliver for the first time an innovative, convenient, and highly versatile biosensor for efficient screening and evaluation of mAbs as antiviral immunotherapies for COVID-19. To demonstrate the capabilities of our innovative technology, we analyze the interaction of inactivated SARS-CoV-2 viruses of different variants with an ACE2-functionalized membrane and the neutralizing effect of different dosage of monoclonal antibodies. Our biomimetic sensor enables a rapid comparison of different antibody candidates as well as different virus variants, and it can provide accurate data on the optimum inhibition concentration (IC_{50}). The new methodology demonstrated here could position biosensor technologies beyond the state of the art – mainly focusing in diagnostic detection analysis and biomolecular interaction characterization – by providing a versatile and powerful device to be employed for the evaluation of novel biomolecular therapy formulations (e.g., nanobodies), for diagnostic seroneutralization assays, for vaccine development, etc. We foresee the implementation of plasmonic biosensors in biomedical and pharmaceutical laboratories as a valuable tool to accelerate, simplify, and reduce costs in the development of more effective, personalized, and universal therapies that can boost healthcare around the world.

2. Experimental section

2.1. Chemical and biological reagents

Acetone and ethanol were purchased from Panreac Applichem (Barcelona, Spain). Lipids (POPC, 1-palmitoyl-2-oleoyl-snglycero-3-phosphocholine) and DOPS (1,2-dioleoyl-sn-glycero-3-phospho-L-serine) were provided by Avanti Polar Lipids (Alabaster, Alabama, USA). Reagents for buffer preparation (10 mM PBS (Phosphate buffer saline, pH 7.4), 50 mM HEPES (N-(2-Hydroxyethyl) piperazine-N-(2-ethanesulfonic acid, pH 7.24), and MES (2-(N-morpholino) ethane sulfonic acid, pH 5.0)) and reagents for carboxylic groups activation (1-ethyl-3(3- dimethylaminopropyl) carbodiimide hydrochloride (EDC) and sulfo-N-hydroxysuccinimide (s-NHS)) were purchased to Sigma-Aldrich (Steinhem, Germany). Angiotensin-converting enzyme 2 (ACE-2), SARS-CoV-2 S proteins, and neutralizing monoclonal antibody 2 (NAb2) were acquired from GenScript (Leiden, The Netherlands). The neutralizing monoclonal antibody 1 (Nab1) was acquired from Sino Biologicals (Eschborn, Germany). The inactivated SARS-CoV-2 viruses Omicron BA.1 (hCoV-19/Italy/LAZ-INMI-2890/2021, GISAID accession ID EPI_ISL_7716384) and B1.617.2/delta (hCoV-19/Italy/LAZ-INMI-648/2021 GISAID accession ID EPI_ISL_2000624) were kindly provided by our collaborator Dr. Giulia Matusali from The National Institute of Infectious Diseases Lazzaro Spallanzani (INMI, Rome, Italy). The virus production and inactivation procedures have been described in (Ruiz--Vega et al., 2022).

2.2. SPR biosensor description

Our proprietary SPR biosensor based on Kretschmann configuration is a self-designed and assembled compact and small device able to monitor binding events in real-time through resonance wavelength interrogation at a fixed angle of incidence ($\theta = 70^o$). The plasmonic sensor chip is sandwiched in between a trapezoidal glass prism linked through a refractive index matching oil ($n = 1.512$) and a customized polymeric single-channel flow cell. The flow cell is connected to a fluidic delivery system composed of a syringe pump and a hand-functioned injection valve including a loop (150 μL) for sample injection. The syringe pump delivers a constant volume flow at a fixed rate that can be adjusted. A collimated TM-polarized broadband light source is used to excite the sensor surface through prism coupling and the reflected light is collected and fiber-coupled to a CCD mini-spectrometer (Jaz Module, Ocean Optics, Orlando, FL, USA). The real-time monitoring of shifts in plasmonic resonance peak (λ_{SPR}) can be read out by polynomial fitting using a user-friendly home-made software developed in open-source programming scripts (Python). Au plasmonic thin films (1 nm Ti, 49 nm Au) were coated with a thin layer of SiO2 (10 nm) to provide a hydrophilic surface for efficient lipid bilayer formation. Before mounting the plasmonic chip on the SPR sensor, a specific protocol for chip cleaning was followed. Firstly, the chip was sonicated 1 min at room temperature in various solvents acetone, ethanol, and MiliQ water, respectively, then dry with an N_2 stream. To make the sensor surface more hydrophilic, the plasmonic chip was placed in UV/Ozone Procleaner Plus (Bioforce Nanosciences, Utah, US) for 30 min. Optical characterization of the SPR biosensor is detailed in the Supporting Information (Fig. S1).

2.3. Supported lipid bilayer (SLB) formation and ACE-2 receptor immobilization

The functional supported lipids bilayer (SLB) was formed by disruption of small unilamellar vesicles (SUV) over a hydrophilic SiO_2 surface. A specific volume of different lipid formulations (POPC:DOPS, 10:1) was dissolved in chloroform and mixed in a glass vial to obtain 1 mg of dry lipids. To evaporate the solvent residues and form a dry lipids thin film, the vial was stored in a vacuum desiccator overnight in continuous N_2 flux at room temperature. To rehydrate the lipid's thin film, 1 mL PBS buffer (10 mM, pH 7.4) was added up to get 1 mg/mL concentration. The final solution was vortexed for 2–3 min and sonicated at room temperature for 1 h to make a heterogenous vesicles solution. The vesicles were extruded into small unilamellar vesicles (SUVs) through a polycarbonate membrane pore size (0.1 μm) with 100

extrusion cycles at 60° °C temperature by using a mini-extruder (Avanti Polar Lipids, Inc., Alabaster, AL, USA). The final SUV solution was quickly injected through the sensor surface to create a lipids bilayer on SiO_2-coated Au thin film. After, a cleaning step of 10 mM NaOH was carried out to ensure a stable formation of a planar lipid layer. Once the functional SLB layer was stabilized, angiotensin-converting enzyme 2 receptors fused to a human Fc recombinant molecule (ACE-2, 50 μg/mL) were covalently anchored through EDC/NHS (0.4 M/0.1 M) chemistry onto the functional SLB layer in MES buffer (50 mM, pH 5). To deactivate the unreacted COOH groups, ethanolamine (EA, 1 M, pH 8) was injected for 1 min. All the measurements were carried out with PBS as running buffer at 20 μL/min flow rate.

2.4. SARS-CoV-2 virus detection and neutralization assays

The optimization and evaluation of the virus detection assay were performed with the biomimetic ACE-2 functionalized sensor chip employing two variants of SARS-CoV-2: Delta and Omicron (using the viral antigens and whole UV-inactivated SARS-CoV-2 virus). The calibration curves for both viral antigens and whole viruses were generated by measuring concentrations ranging from 30 ng/mL to 5000 ng/mL and 10^3 TCID50/mL to 5×10^5 TCID50/mL, respectively, in standard buffer (HEPES, 50 mM, pH 7.4) at 20 μL/min flow rate. After each sample, the receptor-analyte interactions were disrupted and the biosurface was regenerated by injecting 10 mM NaOH solution for 2 min at the same flow rate. For neutralization assays, virus samples containing the mAbs at different concentrations (from 0 to 5000 ng/mL) were pre-incubated for 10 min at room temperature and then flowed over the biofunctionalized surface. Data were analyzed using Origin 8.0 (OriginLab, MA, US) and GraphPad Prism 8 (GraphPad Software, CA, US). Detection calibration curves were plotted as the mean and standard deviation (mean ± SD) of the acquired biosensor response (Δλ) *versus* the target concentration. The data were fitted to a two-site specific binding model curve. The limit of detection (LOD), defined as the smallest concentration distinguishable from the blank, and the limit of quantification (LOQ), defined as the minimum concentration that can be reliably detected and quantified, were determined as the concentration corresponding to 3 and 10 times the standard deviation of the baseline of the sensor signal, respectively. Inhibition calibration curves were plotted as the mean and standard deviation of the biosensor response normalized to percentages. The data were fitted to a dose-response inhibition fitting curve. The half maximal inhibitory concentration (IC_{50}) can be defined as the 50% quantity of drug required to inhibit a biological process. This value can be calculated by testing different analyte concentrations in triplicates and signals (mean ± SD) plotted *vs* the logarithmic value of the analyte concentration. All experiments for the virus detection were carried out in the ICN2 BSL2 facilities with approval of the Biosafety Committee of the Autonomous University of Barcelona (UAB) (HR-599-20).

3. Results and discussion

3.1. Formation of artificial cell membranes expressing ACE-2 receptors

We have employed a custom-designed proprietary SPR biosensor based on prism-coupling excitation and wavelength interrogation for the creation of an artificial host cell interface displaying ACE-2 receptors, which provides a nature-imitating scaffold for therapeutic mAb evaluation through SARS-CoV-2 neutralization assays. This biosensor provides label-free and real-time monitoring of biological interactions with excellent sensitivity in a user-friendly environment and operation. Our biosensor technology has previously proved itself as a potential candidate for clinical diagnostics and biomedical research, including direct detection of proteins (Aviñó et al., 2019; Calvo-Lozano et al., 2022; Pelaez et al., 2020; Soler et al., 2016b, 2015, 2014), nucleic acids (Calvo-Lozano et al., 2020; Huertas et al., 2018, 2016), and small molecules (Peláez et al., 2020, 2018; Soler et al., 2016a) for different applications, generally employing a functional chemical matrix based on alkanethiol self-assembled monolayers (SAMs) for direct gold sensor surface functionalization. In this work, the formation of artificial cell membranes based on supported lipids bilayer (SLB) replaces the rigid SAMs, providing a 2D biomimetic scaffold that allows a slight bioreceptor lateral mobility to form clusters and enhancing cell-cell interactions (Soler et al., 2018).

Planar and functional SLBs can be formed onto the sensor surfaces through a well-established methodology based on spontaneous disruption of small unilamellar vesicles (SUV) upon contact with hydrophilic surfaces, like SiO_2 (Hardy et al., 2013; Kilic and Kok, 2016; Neupane et al., 2018; Richter and Brisson, 2005). In this sense, we have included a 10 nm SiO_2 coating on the gold sensors, which will ensure the long-term hydrophilicity of the substrate and the stability of the lipid layer (Fig. 2a) (Ulmefors et al., 2021). The large variety of existing lipid formulations allows preparing vesicles with different mixtures that incorporate desired functionalities (e.g., amine, carboxyl, biotin, etc.) for subsequent conjugation with the cell receptor. We have selected a mixture of phosphocholine (1-palmitoyl-2-oleoyl-snglycero-3-phosphocholine, POPC) at 90% molar ratio with a carboxyl (-COOH) functional phosphoserine (1,2-dioleoyl-sn-glycero-3-phospho-L-serine, DOPS) at 10% molar ratio. SUVs were prepared by extrusion, employing 0.1 μm size filtration membranes, resulting in an homogeneous suspension of approximately 100 nm vesicles in PBS buffer. The SUV suspension was readily injected on the SPR biosensor and the formation of the SLB onto the sensor surface was monitored in real time (Fig. 2b). The sharp increase of the sensor response (corresponding to a cooperative binding equation), reached equilibrium at $\Delta\lambda = 14$ nm, indicating that SUVs instantly disrupted over the sensor surface and promptly formed a uniform SLB layer. A cleaning solution (NaOH 10 mM) was flowed over the bilayer for 2 min to confirm stability (i.e., nothing was removed from the surface). After, we covalently immobilized ACE-2 receptors (50 μg/mL) on the COOH-functional SLB by means of the well-known EDC/NHS chemistry (Fig. 2c). We employed a recombinant human ACE-2 – Fc chimera in order to facilitate its anchoring onto the lipid surface and ensure accessibility of the viruses. The whole biofunctionalization procedure was carried out *in situ* at room temperature and was completed within approximately 2 h. To confirm the robustness and reproducibility of the procedure for artificial cell membrane formation, we determined the coefficient of variability for both SLB formation and ACE-2 immobilization, obtaining values of 7% and 14%, respectively, over more than 25 biofunctionalization processes.

3.2. Analysis of SARS-CoV-2 virus interaction with ACE-2 cell receptors

The artificial cell membrane scaffold prepared on the plasmonic sensor surface was first used to study and evaluate the binding interaction between the ACE-2 receptors and the SARS-CoV-2 viruses of both variants. Initially, we employed recombinant viral antigens corresponding to the Spike (S) protein of Delta and Omicron SARS-CoV-2 to confirm specific detection of the viruses and to assess possible affinity differences between the two variants (Fig. 3a and Fig. S2). The calibration curves for SARS-CoV-2 viral antigens over a wide range of concentrations (15–5000 ng/mL) were plotted against the biosensor response (Δλ); the limits of detection (LOD) and limits of quantification (LOQ) were determined at 18 ng/mL and 49 ng/mL, respectively, for the Delta variant, and at 12 ng/mL and 37 ng/mL, respectively, for the Omicron variant. These excellent sensitivity values prove the powerful performance of the SPR biosensor for highly accurate biomolecular detection assays, and indicate no major affinity differences of the ACE-2 receptor towards the two virus variants.

Since our main goal is to develop a close-to-nature biomimetic assay, we also employed inactivated SARS-CoV-2 viruses as main target. The SARS-CoV-2 viruses were produced and provided by the National Institute of Infectious Diseases (INMI) of Rome (Italy), and they were

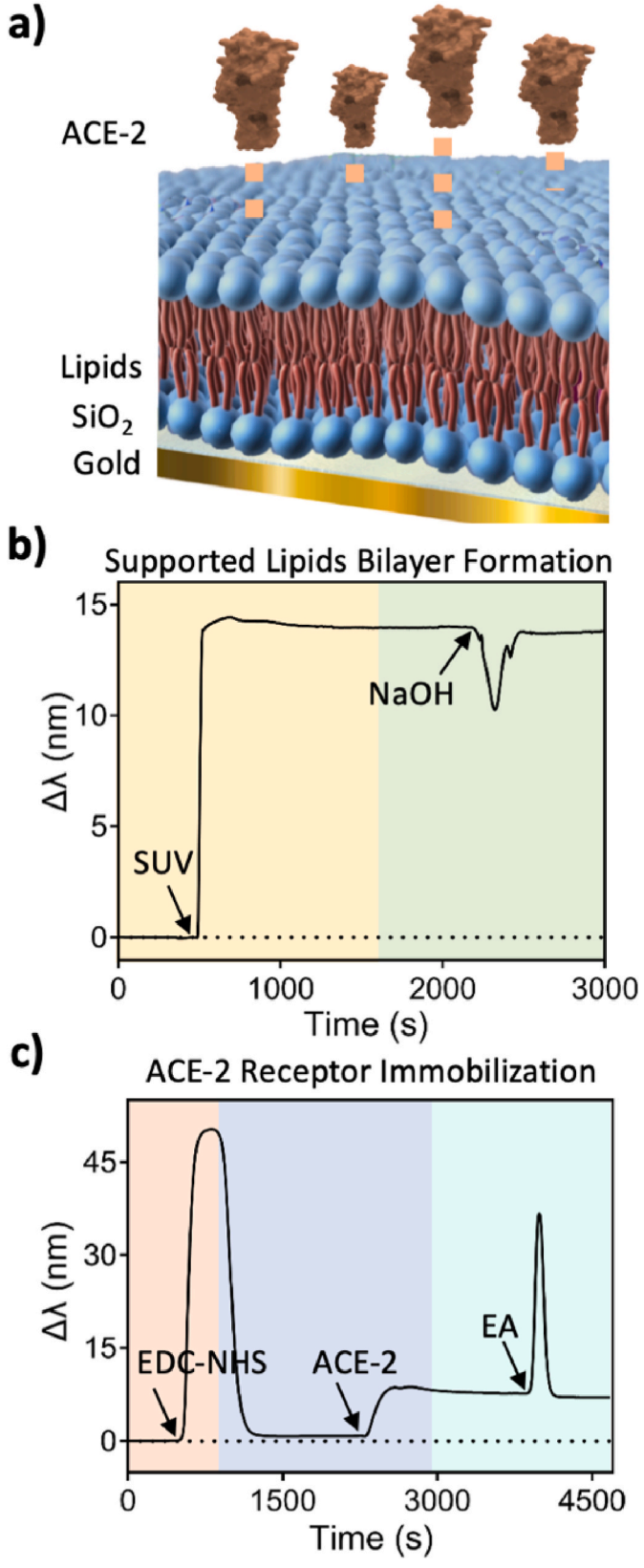

Fig. 2. **(a)** Schematic illustration of the ACE-2 functional supported lipid bilayer formed on SiO_2-coated plasmonic sensor surface; **(b)** SPR sensorgram showing the formation of a lipid bilayer from the disruption of small unilamellar vesicles (SUV), followed by a NaOH cleaning step; **(c)** SPR sensorgram showing the ACE-2 receptor immobilization on the COOH-functional SLB.

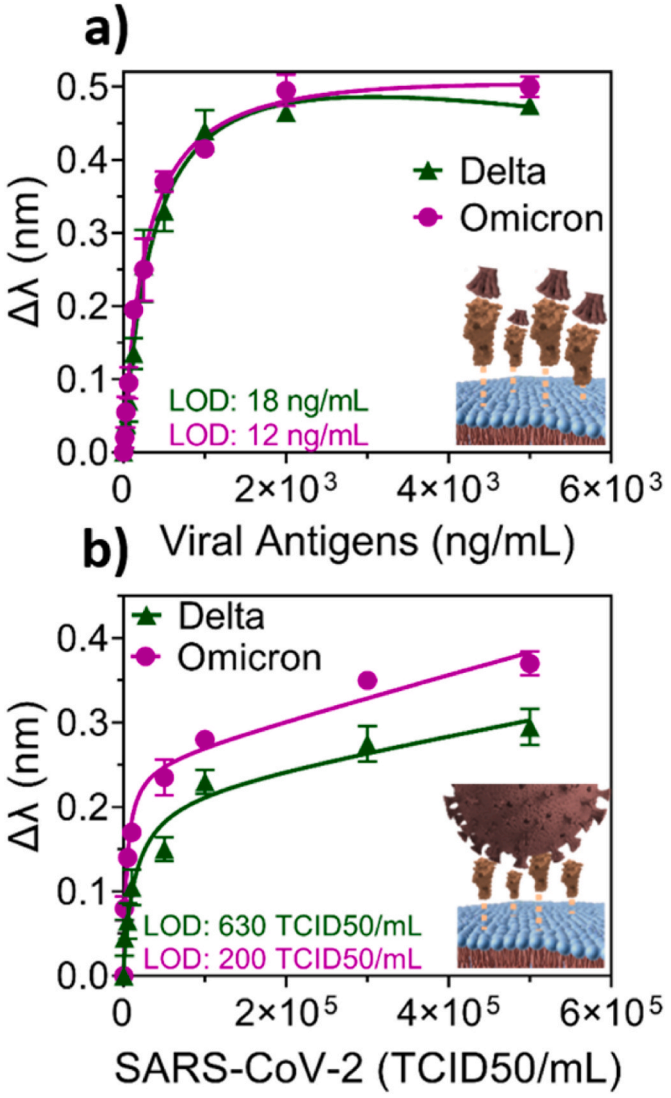

Fig. 3. Standard calibration curve for **a)** SARS-CoV-2 viral antigens (Delta and Omicron) obtained with triplicate measurements of different concentrations over a range between 30 ng/mL to 5000 ng/mL for each specific protein variant; and **b)** UV-inactivated SARS-CoV-2 virus different variants (delta and omicron) obtained with triplicate measurements of different virus titters over a range between 10^3 TCID50/mL to 5×10^5 TCID50/mL for each specific virus variant.

duly inactivated through ultraviolet (UV) irradiation (15 min, λ 254 nm), which was verified by inoculating the viruses on VeroE6 cells and confirming no viral replication for three consecutive passages. The UV inactivation treatment is intended to only affect the genomic material of the virus (RNA), therefore unaltering the external structure of the viral particles allowing their safely use in BSL2 laboratories (Ruiz-Vega et al., 2022). SARS-CoV-2 samples at different titers (10^3 to 5×10^5 TCID50/mL) were prepared by serial dilution in standard buffer (HEPES 50 mM pH 7.4) and flowed over the biomimetic scaffold on the sensor surface. We obtained calibration curves for the Delta and Omicron variants, showing a proportional increase of the sensor signal with the viral load (Fig. 3b and Fig. S2). The LODs were determined at 630 TCID50/mL and 200 TCID50/mL for Delta and Omicron variants, respectively. The LOQs were determined at 4700 TCID50/mL and 1200 TCID50/mL for Delta and Omicron variants, respectively. Here, we perceived that the binding of Omicron SARS-CoV-2 viruses to the ACE-2 receptor is slightly better (25% higher binding efficacy) than the Delta SARS-CoV-2 virus. The reason could be attributed to the spontaneous

mutations occurred within the Omicron S protein, presenting a higher affinity towards the cell receptors, becoming more contagious, as it has been observed during the evolution of the COVID-19 pandemic. Nonetheless, it could also be due to unavoidable experimental variations in the production, inactivation, or manipulation of the viral samples during the study. The sensitivity values obtained for the direct and label-free detection of SARS-CoV-2 viruses with our novel biomimetic sensor are outstanding compared to the state-of-the-art. To our knowledge, only a recent study has reported a plasmonic sensor for the quantification of whole SARS-CoV-2 virus particles, achieving a detection limit of 370 viral particles per mL (vp/mL) (Huang et al., 2021), which is within the same range of our approach but using pseudotyped viruses, a secondary amplification step with gold nanoparticles, and not validated with real samples. On the other hand, our group developed a nanophotonic interferometric sensor for COVID-19 diagnostics demonstrating direct SARS-CoV-2 virus detection with detection limits below 100 TCID50/mL (Ruiz-Vega et al., 2022). Herein, we have achieved similar results employing a conventional and user-friendly SPR technology with an innovative sensor biofunctionalization, which is considered to enhance the SARS-CoV-2 virus binding interaction by mimicking the human cell micro-environment. In fact, different experiments performed for the detection of SARS-CoV-2 viruses using conventional biofunctionalization with self-assembled monolayers resulted in lower sensitivity and worse reproducibility (see Supporting Information, Fig. S3). Furthermore, it is important to remark that the range of virus concentrations employed in this study correspond to most common viral loads found in COVID-19 patients at early stages of the infection (Caplan et al., 2021; Soria et al., 2021), being therefore appropriate for the evaluation of antiviral therapies for early treatment.

3.3. Evaluation of binding affinity and neutralization capacity of different monoclonal antibodies with SARS-CoV-2 viral antigens

For the development of the biosensor-based neutralization assay, we selected two different commercial SARS-CoV-2 neutralizing mAbs (NAb): NAb1, which is a recombinant IgG produced towards the wild-type SARS-CoV-2 Spike protein (S1 fraction) and the NAb2, which is a recombinant IgM produced against a recombinant SARS-CoV-2 RBD protein. A preliminary evaluation study was carried out to test and confirm the reactivity and affinity of both NAb towards the two variants of the SARS-CoV-2 virus. To that, we prepared a SPR sensor chip functionalized with each viral antigen (Delta-S protein and Omicron-S protein), immobilized onto a conventional alkanethiol SAM through EDC/NHS chemistry. Various concentrations of NAb1 and NAb2, in the range of 15 ng/mL to 200 ng/mL, were flowed over each immobilized viral antigen to obtain concentration-dependent binding curves (Fig. 4a and b). We also tested a negative control sample (SARS-CoV-2 Nucleocapside (N) protein at 200 ng/mL) that resulted in negligible non-specific interaction with each viral antigen. These binding curves demonstrate an appropriate affinity of both neutralizing antibodies towards each viral antigens, and therefore their capability to interfere in the interaction between the virus and the cell receptor to prevent infection (Xiaojie et al., 2021).

Once the affinity and binding interaction of the neutralizing antibodies with the target viral antigens was confirmed, we proceeded to perform competitive immunoassays with the same recombinant viral antigens in order to test and evaluate the effectiveness of the antibodies to inhibit the interaction with the cell receptor immobilized on the artificial cell membrane (Fig. 5a). Different dilutions of NAb1 and NAb2 (7.8–5000 ng/mL) were incubated for 10 min with Delta S-protein and Omicron S-protein, respectively, at a fixed concentration (500 ng/mL) (Fig. 5b and c). Representative sensorgrams are shown in Supporting Information (Fig. S4). We also included a blank sample (viral antigen sample with no NAb), and a negative control sample (NAb at 5000 ng/mL with no viral antigen), which resulted in null or negligible signal. As expected, in all cases, the presence of neutralizing antibodies was able to

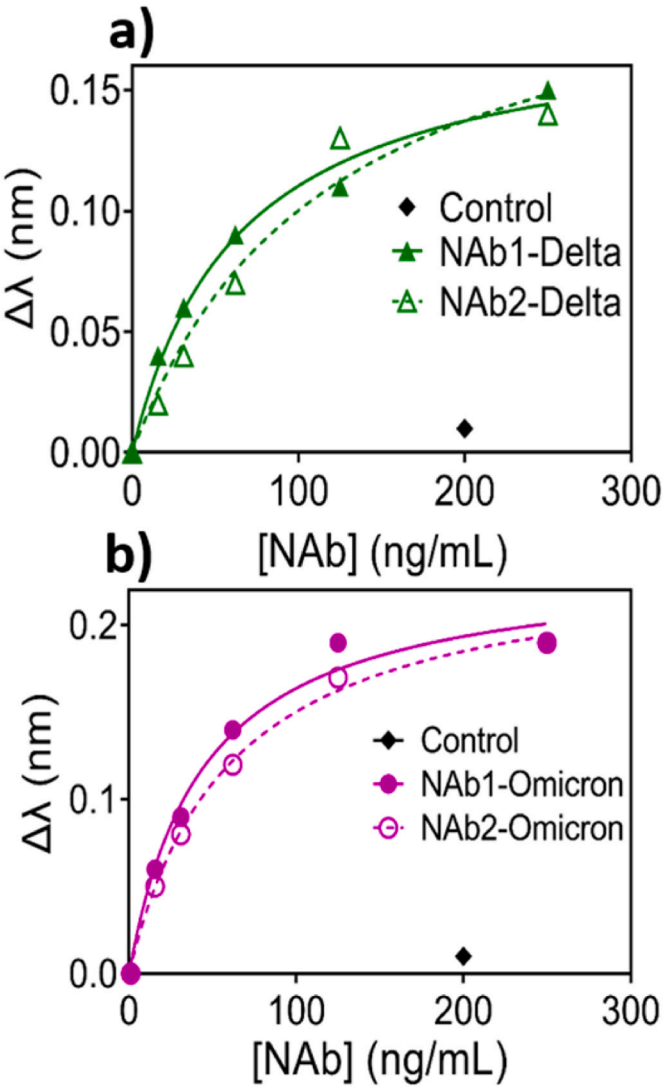

Fig. 4. a) binding curves for Delta-S protein with NAb1 and NAb2, respectively; and **b)** Standard binding curves for Omicron-S protein with NAb1 and NAb2, respectively.

reduce and eventually impede the interaction of the viral antigens with the immobilized ACE-2 receptor, achieving complete blocking of the interaction at concentrations higher than 2000 ng/mL. Slight differences could be readily observed when comparing the two different NAbs, as the assays with NAb2 (neutralizing IgM) resulted in an early reduction of the signal compared to the assays with NAb1 (neutralizing IgG). These differences were corroborated with the determination of the half maximum inhibition concentration (IC_{50}); for the Delta variant assay, the IC_{50} (NAb1) was 142 ng/mL, while the IC_{50} (Nab2) was 68 ng/mL, and for the Omicron variant assay, the IC_{50} (Nab1) was 122 ng/mL and the IC_{50} (Nab2) was 39 ng/mL. These results could be explained by intrinsic structural differences between both Nabs. An IgG is a Y-shaped bivalent molecule with 2 antigen binding sites at their short arms, while an IgM is a pentamer biomolecule with up to 10 antigen binding sites. It can be therefore assumed that IgMs would be more efficient to trap viral antigens in solution, and therefore able to accelerate the blocking of their interaction with ACE-2 receptors.

3.4. Demonstration and validation of the biomimetic SPR neutralization assays for SARS-CoV-2 viruses with different neutralizing antibodies

Finally, we addressed the validation of our biomimetic plasmonic

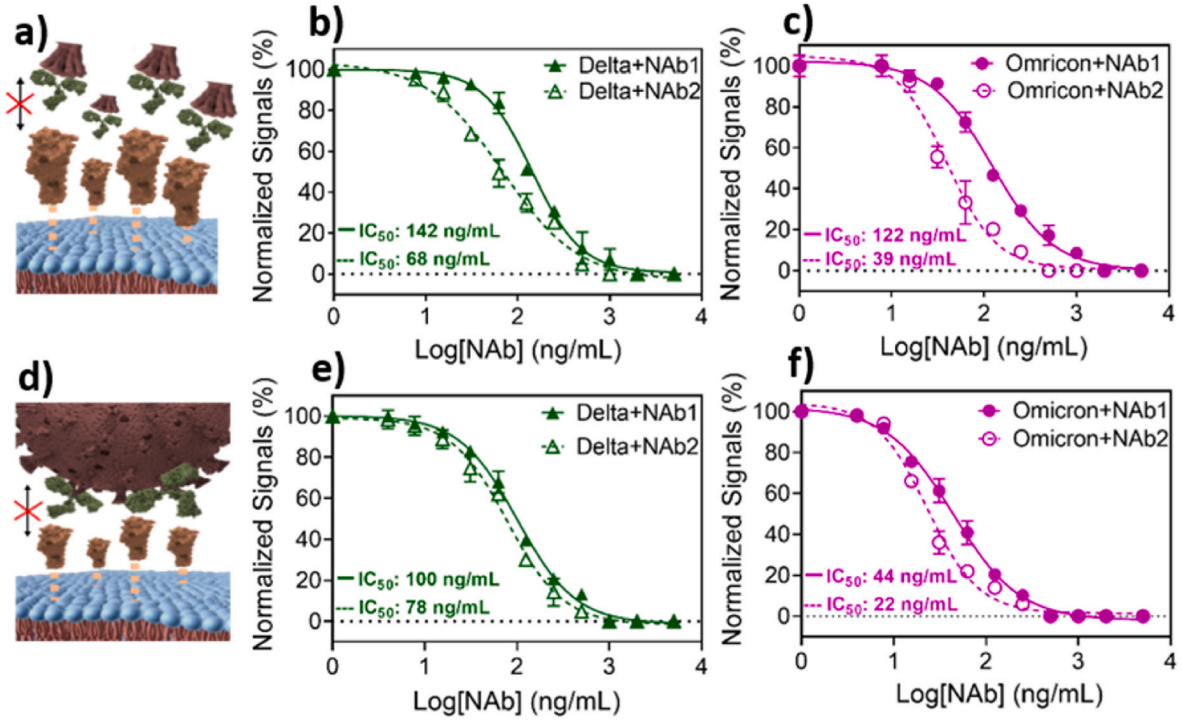

Fig. 5. Competitive immunoassay with SARS-CoV-2 viral antigens and virus variants: **a)** Schematic illustration of the neutralization assay performed with SARS-CoV-2 viral antigens and neutralizing antibodies (NAb) over an ACE-2 receptor anchored to a SLB-functionalized SPR biosensor; **b)** Inhibition curves obtained for the Delta-S protein at a fixed concentration (500 ng/mL) incubated with different concentrations of both neutralizing antibodies (NAb1 and NAb2); **c)** Inhibition curves obtained for the Omicron-S protein at a fixed concentration (500 ng/mL) incubated with different concentrations of both neutralizing antibodies (NAb1 and NAb2). All sensor signals are normalized according to maximum signal (100%) and minimum signal (0%) to facilitate comparison; **d)** Schematic illustration of the neutralization assay performed with SARS-CoV-2 viruses and neutralizing antibodies (NAb) over an ACE-2 receptor anchored to a SLB-functionalized SPR biosensor; **e)** Inhibition curves obtained for the Delta SARS-CoV-2 at a fixed concentration (5×10^4 TCID50/mL) incubated with different concentrations of both neutralizing antibodies (NAb1 and NAb2); **f)** Inhibition curves obtained for the Omicron SARS-CoV-2 viruses at a fixed concentration (5×10^4 TCID50/mL) incubated with different concentrations of both neutralizing antibodies (NAb1 and NAb2). All sensor signals are normalized according to maximum signal (100%) and minimum signal (0%) to facilitate comparison.

sensor for the evaluation of neutralizing mAbs with the SARS-CoV-2 viruses. The virus competitive immunoassays were carried out similarly to the ones performed with viral antigens. A fixed concentration of UV-inactivated SARS-CoV-2 virus sample (5×10^4 TCID50/mL) was incubated with different concentrations of NAb1 and NAb2 (7.8–5000 ng/mL) for 10 min, and then directly introduced in the sensor functionalized with an artificial cell membrane displaying ACE-2 receptors (Fig. 5d). Dose-response inhibition curves were obtained for each SARS-CoV-2 variant (Delta and Omicron) and for each neutralizing antibody (Fig. 5e and f). Representative sensorgrams are shown in Supporting Information (Fig. S5). The IC_{50} values for each assay were calculated at 100 ng/mL and 78 ng/mL for the Delta variant with NAb1 and NAb2, respectively; and 44 ng/mL and 22 ng/mL for the Omicron variant with NAb1 and NAb2, respectively (Table 1). Herein, the differences between the two NAbs are not significant, compared to the 3D neutralization assay performed with viral antigens in solution, which reveals the importance of carrying out the assays in a biomimetic manner, with both ACE-2 receptor and Spike proteins embedded in their corresponding cell membranes. Despite the fact that NAb2 is an IgM molecule with more binding sites available, the steric hindrance limits its capability to interact with a large number of antigens and the inhibition capability results similar to the one of the IgG antibodies. On the other hand, the superior capability of both antibodies for neutralizing the Omicron variant more efficiently than the Delta variant is maintained, with overall lower IC_{50} values and achieving a complete inhibition of the interaction with a lower dose (approximately 250 ng/mL).

Table 1
Summary of main analytical parameters.

SARS-CoV-2 target and variant	Direct & Label-free Detection		Neutralization Assay	
	LOD	LOQ	IC50 (NAb1)	IC50 (NAb2)
Delta S protein	18 ng/mL	49 ng/mL	142 ng/mL	68 ng/mL
Omicron S protein	12 ng/mL	36 ng/mL	122 ng/mL	39 ng/mL
Delta SARS-CoV-2 virus	630 TCID50/mL	4.8×10^3 TCI50/mL	100 ng/mL	78 ng/mL
Omicron SARS-CoV-2 virus	200 TCI50/mL	1.2×10^3 TCI50/mL	44 ng/mL	22 ng/mL

The comparison of this study with those performed for some of the approved mAb immunotherapies, such as casirivimab, imdevimab, bamlanimab and sotrovimab, shows that the IC_{50} values determined in our biomimetic sensing assay are in good agreement with the values determined through standard techniques (ELISA), which range between 10 and 1000 ng/mL (Hwang et al., 2022), confirming the accuracy of the analysis. Furthermore, it is important to remark that the biomimetic SPR sensor offers key advantages over the conventional techniques, like the rapidness and possibility to automate the assays - with no need of amplification, washing, or labelling processes -, the reliability of performing close-to-nature analysis without the complex and time-consuming mammalian cell culturing, and employing a small volume of virus sample (150 μL) at concentrations analogue to common viral loads found in patients with mild or moderate symptomatology. All these characteristics become critical when addressing the evaluation of novel therapeutic candidates, and especially in a global health emergency like the COVID-19 pandemic. The possibility to perform simpler, reagent-less, faster, and more reliable therapy screening and assessment

studies could readily accelerate the selection and regulation of the most promising formulations, reducing the production and manufacturing costs, and boosting their implementation in healthcare systems worldwide.

4. Conclusions

We have developed a rapid, simple and user-friendly biomimetic sensing assay to reduce the overall complexity of SARS-CoV-2 neutralization studies and to accelerate the production and optimization of new COVID-19 immunotherapies based on monoclonal antibodies. Our plasmonic sensor is functionalized with an artificial cell membrane that imitates the real virus-cell interactions, enabling label-free monitoring of the biomolecular infection mechanism (SARS-CoV-2 S protein binding to ACE-2 receptor) in real time, without introducing external tags, and reaching an excellent sensitivity, with detection limits in the 10^2 TCID50/mL range for two major variants of concern of SARS-CoV-2 viruses (Delta and Omicron), which is one order of magnitude better than the majority of plasmonic biosensors reported so far (10^3–10^4 viruses/mL). The biomimetic sensor has been applied for the evaluation of two different monoclonal antibodies as potential candidates for early COVID-19 treatment. The neutralization sensing assays performed with real inactivated SARS-CoV-2 viruses have allowed for the determination of IC_{50} values within the same range of those determined for already approved mAb therapies. Compared to conventional techniques based on biomolecular immunoassays or cell culture methods, our approach enables an accurate and reliable study of the affinity and neutralization capabilities of antibodies towards SARS-CoV-2 in a label-free and real-time format, employing only a low-volume sample of viruses at realistic titers for their ultimate application as early treatment in non-hospitalized COVID-19 patients with mild-moderate symptomatology. These outcomes demonstrate the potential of the new biomimetic sensor technology as a convenient platform for the evaluation of other types of antibodies or immunotherapies for upcoming SARS-CoV-2 variants or other infectious diseases, autoimmune disorders, or cancer. As future perspective, we foresee the implementation of these biosensors as a simple and reliable technology that could be used in biomedical and pharmaceutical laboratories to boost the development and administration of novel therapies at a global scale.

CRediT Author Statement

Razia Batool carried out the experiments and data analysis. Maria Soler conceived and designed the project, supervised the experiments and carried out data analysis and discussion. RB and MS prepared the manuscript. INMI produced and purified the UV-inactivated SARS-CoV-2 samples. LML coordinates the research and supervised experimental and discussion activities. All authors have read, revised, and approved the final version of the manuscript.

Declaration of competing interest

The authors declare that they have no known competing financial interests or personal relationships that could have appeared to influence the work reported in this paper.

Data availability

Data will be made available on request.

Acknowledgments

Financial support is acknowledged from the SensCELL project (Ref. No. PGC-2018-099870), funded by the Spanish Ministry of Science and Innovation (MCIN), the Spanish Research Agency (AEI), and the European Regional Development Fund (ERDF), and from the CONVAT project (Ref. 101003544), funded by the H2020 Research and Innovation Programme of the European Commission (H2020-SC1-PHE-Coronavirus-2020). RB acknowledges the economic support (Ref. PRE2019-089357) from MCIN and AEI linked to the project SEV-2017-0706-19-4. MS acknowledges the economic support of the Ramon y Cajal Grant (RYC2020-029015-I) funded by the AEI/MCIN and the European Union NextGenerationEU/PRTR. INMI also acknowledges funding from the European Virus Archive – GLOBAL (Grant No. 871029). The ICN2 is supported by the CERCA programme (Generalitat de Catalunya) and the Severo Ochoa Centres of Excellence programme, funded by the AEI (Grant. No. SEV-2017-0706).

Appendix A. Supplementary data

Supplementary data to this article can be found online at https://doi.org/10.1016/j.bios.2023.115137.

References

AminJafari, A., Ghasemi, S., 2020. The possible of immunotherapy for COVID-19: a systematic review. Int. Immunopharm. 83, 106455 https://doi.org/10.1016/j.intimp.2020.106455.

Aviñó, A., Jorge, A.F., Huertas, C.S., Cova, T.F.G.G., Pais, A., Lechuga, L.M., Eritja, R., Fabrega, C., 2019. Aptamer-peptide conjugates as a new strategy to modulate human α-thrombin binding affinity. Biochim. Biophys. Acta Gen. Subj. https://doi.org/10.1016/j.bbagen.2019.06.014.

Behrouzi, K., Lin, L., 2022. Gold nanoparticle based plasmonic sensing for the detection of SARS-CoV-2 nucleocapsid proteins. Biosens. Bioelectron. 195, 113669 https://doi.org/10.1016/j.bios.2021.113669.

Calvo-Lozano, O., Aviñó, A., Friaza, V., Medina-Escuela, A., Huertas, C.S., Calderón, E.J., Eritja, R., Lechuga, L.M., 2020. Fast and accurate pneumocystis pneumonia diagnosis in human samples using a label-free plasmonic biosensor. Nanomaterials 10 (1246 10), 1246. https://doi.org/10.3390/NANO10061246, 2020.

Calvo-Lozano, O., Sierra, M., Soler, M., Estévez, M.C., Chiscano-Camón, L., Ruiz-Sanmartin, A., Ruiz-Rodriguez, J.C., Ferrer, R., González-López, J.J., Esperalba, J., Fernández-Naval, C., Bueno, L., López-Aladid, R., Torres, A., Fernández-Barat, L., Attoumani, S., Charrel, R., Coutard, B., Lechuga, L.M., 2022. Label-free plasmonic biosensor for rapid, quantitative, and highly sensitive COVID-19 serology: implementation and clinical validation. Anal. Chem. 94, 975–984. https://doi.org/10.1021/ACS.ANALCHEM.1C03850/ASSET/IMAGES/LARGE/AC1C03850_0007 (JPEG).

Caplan, A., Bates, K.W., Brioni, C., Santos, A., Sabatini, L.M., Kaul, K.L., Carnethon, M.R., Khandekar, J.D., Greenland, P., 2021. Clinical characteristics and viral load dynamics of COVID-19 in a mildly or moderately symptomatic outpatient sample. PLoS One 16, e0258970. https://doi.org/10.1371/JOURNAL.PONE.0258970.

Creech, C.B., Walker, S.C., Samuels, R.J., 2021. SARS-CoV-2 Vaccines 325, 1318–1320.

Dahlin, A., Zäch, M., Rindzevicius, T., Käll, M., Sutherland, D.S., Höök, F., 2005. Localised surface plasmon resonance sensing of lipid-membrane-mediated biorecognition events. J. Am. Chem. Soc. 127, 5043–5048. https://doi.org/10.1021/ja043672o.

Dinnes, J., Deeks, J.J., Berhane, S., Taylor, M., Adriano, A., Davenport, C., Dittrich, S., Emperador, D., Takwoingi, Y., Cunningham, J., Beese, S., Domen, J., Dretzke, J., Ferrante di Ruffano, L., Harris, I.M., Price, M.J., Taylor-Phillips, S., Hooft, L., Leeflang, M.M.G., McInnes, M.D.F., Spijker, R., Van den Bruel, A., Arevalo-Rodriguez, I., Buitrago, D.C., Ciapponi, A., Mateos, M., Stuyf, T., Horn, S., Salameh, J.P., McGrath, T.A., van der Pol, C.B., Frank, R.A., Prager, R., Hare, S.S., Dennie, C., Jenniskens, K., Korevaar, D.A., Cohen, J.F., van de Wijgert, J., Damen, J. A.A.G., Wang, J., Agarwal, R., Baldwin, S., Herd, C., Kristunas, C., Quinn, L., Scholefield, B., 2021. Rapid, point-of-care antigen and molecular-based tests for diagnosis of SARS-CoV-2 infection. Cochrane Database Syst. Rev. https://doi.org/10.1002/14651858.CD013705.pub2, 2021.

Drożdżal, S., Rosik, J., Lechowicz, K., Machaj, F., Kotfis, K., Ghavami, S., Łos, M.J., 2020. FDA approved drugs with pharmacotherapeutic potential for SARS-CoV-2 (COVID-19) therapy. Drug Resist. Updates 53, 100719. https://doi.org/10.1016/j.drup.2020.100719.

Hadi, A.G., Kadhom, M., Hairunisa, N., Yousif, E., Mohammed, S.A., 2020. A review on COVID-19: origin, spread, symptoms, treatment, and prevention. Biointerface Res. Appl. Chem. 10, 7234–7242. https://doi.org/10.33263/BRIAC106.72347242.

Hardy, G.J., Nayak, R., Zauscher, S., 2013. Model cell membranes: techniques to form complex biomimetic supported lipid bilayers via vesicle fusion. Curr. Opin. Colloid Interface Sci. 18, 448–458. https://doi.org/10.1016/j.cocis.2013.06.004.

Hassan, M.M., Sium, F.S., Islam, F., Choudhury, S.M., 2021. A review on plasmonic and metamaterial based biosensing platforms for virus detection. Sens. Bio-Sensing Res. 33, 100429 https://doi.org/10.1016/j.sbsr.2021.100429.

Huang, L., Ding, L., Zhou, J., Chen, S., Chen, F., Zhao, C., Xu, J., Hu, W., Ji, J., Xu, H., Liu, G.L., 2021. One-step rapid quantification of SARS-CoV-2 virus particles via low-cost nanoplasmonic sensors in generic microplate reader and point-of-care device. Biosens. Bioelectron. 171, 112685 https://doi.org/10.1016/J.BIOS.2020.112685.

Huertas, C.S., Aviñó, A., Kurachi, C., Piqué, A., Sandoval, J., Eritja, R., Esteller, M., Lechuga, L.M., 2018. Label-free DNA-methylation detection by direct ds-DNA

fragment screening using poly-purine hairpins. Biosens. Bioelectron. 120, 47–54. https://doi.org/10.1016/j.bios.2018.08.027.
Huertas, C.S., Carrascosa, L.G., Bonnal, S., Valcárcel, J., Lechuga, L.M., 2016. Quantitative evaluation of alternatively spliced mRNA isoforms by label-free real-time plasmonic sensing. Biosens. Bioelectron. 78, 118–125. https://doi.org/10.1016/j.bios.2015.11.023.
Hwang, Y.C., Lu, R.M., Su, S.C., Chiang, P.Y., Ko, S.H., Ke, F.Y., Liang, K.H., Hsieh, T.Y., Wu, H.C., 2022. Monoclonal antibodies for COVID-19 therapy and SARS-CoV-2 detection. J. Biomed. Sci. 29, 1–50. https://doi.org/10.1186/s12929-021-00784-w.
Iacob, S., Iacob, D.G., 2020. SARS-CoV-2 treatment approaches: numerous options, No certainty for a versatile virus. Front. Pharmacol. 11, 1–15. https://doi.org/10.3389/fphar.2020.01224.
Kevadiya, B.D., Machhi, J., Herskovitz, J., Oleynikov, M.D., Blomberg, W.R., Bajwa, N., Soni, D., Das, S., Hasan, M., Patel, M., Senan, A.M., Gorantla, S., McMillan, J.E., Edagwa, B., Eisenberg, R., Gurumurthy, C.B., Reid, S.P.M., Punyadeera, C., Chang, L., Gendelman, H.E., 2021. Diagnostics for SARS-CoV-2 infections. Nat. Mater. 20, 593–605. https://doi.org/10.1038/s41563-020-00906-z.
Kilic, A., Kok, F.N., 2016. Biomimetic lipid bilayers on solid surfaces: models for biological interactions. Surf. Innov. 4, 141–157. https://doi.org/10.1680/jsuin.16.00008.
Lei, C., Qian, K., Li, T., Zhang, S., Fu, W., Ding, M., Hu, S., 2020. Neutralization of SARS-CoV-2 spike pseudotyped virus by recombinant ACE2-Ig. Nat. Commun. 11, 1–5. https://doi.org/10.1038/s41467-020-16048-4.
Li, L., Zhang, W., Hu, Y., Tong, X., Zheng, S., Yang, J., Kong, Y., Ren, L., Wei, Q., Mei, H., Hu, C., Tao, C., Yang, R., Wang, Jue, Yu, Y., Guo, Y., Wu, X., Xu, Z., Zeng, L., Xiong, N., Chen, L., Wang, Juan, Man, N., Liu, Y., Xu, H., Deng, E., Zhang, X., Li, C., Wang, C., Su, S., Zhang, L., Wang, Jianwei, Wu, Y., Liu, Z., 2020. Effect of convalescent plasma therapy on time to clinical improvement in patients with severe and life-threatening COVID-19: a randomized clinical trial. JAMA, J. Am. Med. Assoc. 324, 460–470. https://doi.org/10.1001/jama.2020.10044.
Limaj, O., Etezadi, D., Wittenberg, N.J., Rodrigo, D., Yoo, D., Oh, S.-H., Altug, H., 2016. Infrared plasmonic biosensor for real-time and label-free monitoring of lipid membranes. Nano Lett. 16, 1502–1508. https://doi.org/10.1021/acs.nanolett.5b05316.
Ludwig, S., Zarbock, A., 2020. Coronaviruses and SARS-CoV-2: a brief overview. Anesth. Analg. 131, 93–96. https://doi.org/10.1213/ANE.0000000000004845.
Mauriz, E., Lechuga, L.M., 2021. Current trends in spr biosensing of sars-cov-2 entry inhibitors. Chemosensors 9. https://doi.org/10.3390/chemosensors9120330.
Mohan, B., Vinod, N., 2020. COVID-19: an insight into SARS-CoV2 pandemic originated at wuhan city in hubei province of China. J. Infect. Dis. Epidemiol. 6 https://doi.org/10.23937/2474-3658/1510146.
Neupane, S., De Smet, Y., Renner, F.U., Losada-Pérez, P., 2018. Quartz crystal microbalance with dissipation monitoring: a versatile tool to monitor phase transitions in biomimetic membranes. Front. Mater. 5, 1–8. https://doi.org/10.3389/fmats.2018.00046.
Nguyen, H.H., Park, J., Kang, S., Kim, M., 2015. Surface plasmon resonance: a versatile technique for biosensor applications. Sensors 15, 10481–10510. https://doi.org/10.3390/s150510481.
Niknam, Z., Jafari, A., Golchin, A., Danesh Pouya, F., Nemati, M., Rezaei-Tavirani, M., Rasmi, Y., 2022. Potential therapeutic options for COVID-19: an update on current evidence. Eur. J. Med. Res. 27, 1–15. https://doi.org/10.1186/s40001-021-00626-3.
Pashaei, M., Rezaei, N., 2020. Immunotherapy for SARS-CoV-2: potential opportunities. Expet Opin. Biol. Ther. 20, 1111–1116. https://doi.org/10.1080/14712598.2020.1807933.
Payne, S., 2017. Methods to study viruses. Viruses 37–52. https://doi.org/10.1016/b978-0-12-803109-4.00004-0.
Peláez, E.C., Estevez, M.C., Domínguez, R., Sousa, C., Cebolla, A., Lechuga, L.M., 2020. A compact SPR biosensor device for the rapid and efficient monitoring of gluten-free diet directly in human urine. Anal. Bioanal. Chem. 412, 6407–6417. https://doi.org/10.1007/S00216-020-02616-6/FIGURES/6.
Pelaez, E.C., Estevez, M.C., Mongui, A., Menéndez, M.-C., Toro, C., Herrera-Sandoval, O. L., Robledo, J., García, M.J., Portillo, P. Del, Lechuga, L.M., 2020. Detection and quantification of HspX antigen in sputum samples using plasmonic biosensing: toward a real point-of-care (POC) for tuberculosis diagnosis. ACS Infect. Dis. 6, 1110–1120. https://doi.org/10.1021/ACSINFECDIS.9B00502.
Peláez, E.C., Estevez, M.C., Portela, A., Salvador, J.P., Marco, M.P., Lechuga, L.M., 2018. Nanoplasmonic biosensor device for the monitoring of acenocoumarol therapeutic drug in plasma. Biosens. Bioelectron. 119, 149–155. https://doi.org/10.1016/J.BIOS.2018.08.011.
Plaze, M., Attali, D., Prot, M., Petit, A.C., Blatzer, M., Vinckier, F., Levillayer, L., Chiaravalli, J., Perin-Dureau, F., Cachia, A., Friedlander, G., Chrétien, F., Simon-Loriere, E., Gaillard, R., 2021. Inhibition of the replication of SARS-CoV-2 in human cells by the FDA-approved drug chlorpromazine. Int. J. Antimicrob. Agents 57, 106274. https://doi.org/10.1016/j.ijantimicag.2020.106274.
Richter, R.P., Brisson, A.R., 2005. Following the formation of supported lipid bilayers on Mica: a study combining AFM, QCM-D, and ellipsometry. Biophys. J. 88, 3422–3433. https://doi.org/10.1529/biophysj.104.053728.
Ruiz-Vega, G., Soler, M., Carmen Estevez, M., Ramirez-Priego, P., Pazos, M.D., Noriega, M.A., Margolles, Y., Francés-Gómez, C., Geller, R., Matusali, G., Colavita, F., Caro, A. Di, Casasnovas, J.M., Fernández, L.A., Lechuga, L.M., 2022. Rapid and direct quantification of the SARS-CoV-2 virus with an ultrasensitive nanobody-based photonic nanosensor. Sensors & Diagnostics 1, 983–993. https://doi.org/10.1039/d2sd00082b.
Saad, Y., Gazzah, M.H., Mougin, K., Selmi, M., Belmabrouk, H., 2022. Sensitive detection of SARS-CoV-2 using a novel plasmonic fiber optic biosensor design. Plasmonics 1–26. https://doi.org/10.1007/s11468-022-01639-2.
Sen-Crowe, B., McKenney, M., Boneva, D., Elkbuli, A., 2020. A state overview of COVID19 spread, interventions and preparedness. Am. J. Emerg. Med. 38, 1520–1523. https://doi.org/10.1016/j.ajem.2020.04.020.
Sheervalilou, R., Shirvaliloo, M., Dadashzadeh, N., Shirvalilou, S., Shahraki, O., Pilehvar-Soltanahmadi, Y., Ghaznavi, H., Khoei, S., Nazarlou, Z., 2020. COVID-19 under spotlight: a close look at the origin, transmission, diagnosis, and treatment of the 2019-nCoV disease. J. Cell. Physiol. 235, 8873–8924. https://doi.org/10.1002/jcp.29735.
Shrivastav, A.M., Cvelbar, U., Abdulhalim, I., 2021. A comprehensive review on plasmonic-based biosensors used in viral diagnostics. Commun. Biol. 4, 1–12. https://doi.org/10.1038/s42003-020-01615-8.
Singh, K.R.B., Rathee, S., Nagpure, G., Singh, J., Singh, R.P., 2022. Smart and emerging nanomaterials-based biosensor for SARS-CoV-2 detection. Mater. Lett. 307, 131092 https://doi.org/10.1016/J.MATLET.2021.131092.
Soler, M., Estevez, M.-C., Moreno, M.D.L., Cebolla, A., Lechuga, L.M., 2016a. Label-free SPR detection of gluten peptides in urine for non-invasive celiac disease follow-up. Biosens. Bioelectron. 79 https://doi.org/10.1016/j.bios.2015.11.097.
Soler, M., Estevez, M.-C., Villar-Vazquez, R., Casal, J.I., Lechuga, L.M., 2016b. Label-free nanoplasmonic sensing of tumor-associate autoantibodies for early diagnosis of colorectal cancer. Anal. Chim. Acta 930. https://doi.org/10.1016/j.aca.2016.04.059.
Soler, M., Estevez, M.C., Alvarez, M., Otte, M.A., Sepulveda, B., Lechuga, L.M., 2014. Direct detection of protein biomarkers in human fluids using site-specific antibody immobilization strategies. Sensors 14, 2239–2258. https://doi.org/10.3390/s140202239.
Soler, M., Huertas, C.S., 2022. Applications of label-free plasmonic biosensors in clinical diagnostics. Ref. Modul. Biomed. Sci. https://doi.org/10.1016/B978-0-12-822548-6.00119-9.
Soler, M., Lechuga, L.M., 2021. Principles, technologies, and applications of plasmonic biosensors. J. Appl. Phys. 129, 111102 https://doi.org/10.1063/5.0042811.
Soler, M., Li, X., John-Herpin, A., Schmidt, J., Coukos, G., Altug, H., 2018. Two-dimensional label-free affinity analysis of tumor-specific CD8 T cells with a biomimetic plasmonic sensor. ACS Sens. 3, 2286–2295. https://doi.org/10.1021/acssensors.8b00523.
Soler, M., Mesa-Antunez, P., Estevez, M.-C., Ruiz-Sanchez, A.J., Otte, M.A., Sepulveda, B., Collado, D., Mayorga, C., Torres, M.J., Perez-Inestrosa, E., Lechuga, L. M., 2015. Highly sensitive dendrimer-based nanoplasmonic biosensor for drug allergy diagnosis. Biosens. Bioelectron. 66, 115–123. https://doi.org/10.1016/J.BIOS.2014.10.081.
Soria, M.E., Cortón, M., Martínez-González, B., Lobo-Vega, R., Vázquez-Sirvent, L., López-Rodríguez, R., Almoguera, B., Mahillo, I., Mínguez, P., Herrero, A., Taracido, J.C., Macías-Valcayo, A., Esteban, J., Fernandez-Roblas, R., Gadea, I., Ruíz-Hornillos, J., Ayuso, C., Perales, C., 2021. High SARS-CoV-2 viral load is associated with a worse clinical outcome of COVID-19 disease. Access Microbiol 3. https://doi.org/10.1099/ACMI.0.000259.
Sparrow, E., Friede, M., Torvaldsen, S., 2017. Blt 16, 178061 235–237.
Syed Nor, S.N., Rasanang, N.S., Karman, S., Zaman, W.S.W.K., Harun, S.W., Arof, H., 2022. A review: surface plasmon resonance-based biosensor for early screening of SARS-CoV2 infection. IEEE Access 10, 1228–1244. https://doi.org/10.1109/ACCESS.2021.3138981.
Szunerits, S., Saada, H., Pagneux, Q., Boukherroub, R., 2022. Plasmonic approaches for the detection of SARS-CoV-2 viral particles. Biosensors 12. https://doi.org/10.3390/bios12070548.
Thapa, S., Singh, K.R.B., Verma, R., Singh, J., Singh, R.P., 2022. State-of-the-Art smart and intelligent nanobiosensors for SARS-CoV-2 diagnosis, 2022 Biosensors 12, 637. https://doi.org/10.3390/BIOS12080637. Page 637 12.
Ulmefors, H., Nissa, J., Pace, H., Wahlsten, O., Gunnarsson, A., Simon, D.T., Berggren, M., Höök, F., 2021. formation of supported lipid bilayers derived from vesicles of various compositional complexity on conducting polymer/silica substrates. Langmuir 37, 5494–5505. https://doi.org/10.1021/acs.langmuir.1c00175.
Wang, H., Li, X., Li, T., Zhang, S., Wang, L., Wu, X., Liu, J., 2020. The genetic sequence, origin, and diagnosis of SARS-CoV-2. Eur. J. Clin. Microbiol. Infect. Dis. 39, 1629–1635. https://doi.org/10.1007/s10096-020-03899-4.
Wouters, O.J., Shadlen, K.C., Salcher-Konrad, M., Pollard, A.J., Larson, H.J., Teerawattananon, Y., Jit, M., 2021. Challenges in ensuring global access to COVID-19 vaccines: production, affordability, allocation, and deployment. Lancet 397, 1023–1034. https://doi.org/10.1016/S0140-6736(21)00306-8.
Xiaojie, S., Yu, L., lei, Y., Guang, Y., Min, Q., 2021. Neutralizing antibodies targeting SARS-CoV-2 spike protein. Stem Cell Res. 50 https://doi.org/10.1016/j.scr.2020.102125.
Yano, T. aki, Kajisa, T., Ono, M., Miyasaka, Y., Hasegawa, Y., Saito, A., Otsuka, K., Sakane, A., Sasaki, T., Yasutomo, K., Hamajima, R., Kanai, Y., Kobayashi, T., Matsuura, Y., Itonaga, M., Yasui, T., 2022. Ultrasensitive detection of SARS-CoV-2 nucleocapsid protein using large gold nanoparticle-enhanced surface plasmon resonance. Sci. Rep. 12, 1–8. https://doi.org/10.1038/s41598-022-05036-x.
Ye, H., Nowak, C., Liu, Y., Li, Y., Zhang, T., Bleris, L., Qin, Z., 2021. Single-Molecule Detection of SARS-CoV-2 by Plasmonic Sensing of Isothermally Amplified Nucleic Acids medRxiv 2021.10.05.21264561.